Published in final edited form as:

Cell Rep. 2014 January 16; 6(1): 141–154. doi:10.1016/j.celrep.2013.12.010.

The RON Receptor Tyrosine Kinase Promotes Metastasis by Triggering MBD4-Dependent DNA Methylation Reprogramming

Stéphanie Cunha[1], **Yi-Chun Lin**[1], **Elizabeth A. Goossen**[1], **Christa I. DeVette**[1], **Mark R. Albertella**[2], **Stuart Thomson**[2], **Mark J. Mulvihill**[2], and **Alana L. Welm**[1,*]

[1]Department of Oncological Sciences, Huntsman Cancer Institute, University of Utah, 2000 Circle of Hope, Salt Lake City, UT 84112, USA

[2]OSI/Astellas, Bioscience Park Drive, Farmingdale, NY 11735, USA

SUMMARY

Metastasis is the major cause of death in cancer patients, yet the genetic and epigenetic programs that drive metastasis are poorly understood. Here, we report an epigenetic reprogramming pathway that is required for breast cancer metastasis. Concerted differential DNA methylation is initiated by the activation of the RON receptor tyrosine kinase by its ligand, macrophage stimulating protein (MSP). Through PI3K signaling, RON/MSP promotes expression of the G:T mismatch-specific thymine glycosylase MBD4. RON/MSP and MBD4-dependent aberrant DNA methylation results in the misregulation of a specific set of genes. Knockdown of MBD4 reverses methylation at these specific loci and blocks metastasis. We also show that the MBD4 glycosylase catalytic residue is required for RON/MSP-driven metastasis. Analysis of human breast cancers revealed that this epigenetic program is significantly associated with poor clinical outcome. Furthermore, inhibition of Ron kinase activity with a pharmacological agent blocks metastasis of patient-derived breast tumor grafts in vivo.

INTRODUCTION

Metastasis is the main cause of death in cancer patients, and there are currently no therapies that specifically prevent the metastatic process or that can cure metastatic disease. Metastasis is a multistep, dynamic process for which the mechanisms remain enigmatic, and a better

*Correspondence: alana.welm@hci.utah.edu.

ACCESSION NUMBERS

All data described in this paper have been deposited in the NCBI Gene Expression Omnibus under the accession numbers GSE52567 and GSE52689.

SUPPLEMENTAL INFORMATION

Supplemental Information includes Supplemental Experimental Procedures, four figures, and one table and can be found with this article online at http://dx.doi.org/10.1016/j.celrep.2013.12.010

AUTHOR CONTRIBUTIONS

A.L.W. and S.C. conceived the project. S.C. designed and performed experimental work and computational analyses. H&E, immunostaining, and xenograft experiments were carried out by Y.-C.L. E.A.G. performed the PI3K/ MAPK inhibitor experiments. C.I.D. performed the Tet repression experiments. M.R.A., M.J.M., and S.T. provided OSI-296 along with prepublication data for its biochemical and pharmacological properties. S.C. and A.L.W. wrote the manuscript.

understanding of specific pathways that facilitate and/or sustain metastasis continues to be required for the development of new treatments. Transcriptional profiling has clearly demonstrated that there are sets of genes, or “signatures,” expressed in primary tumors that correlate with metastasis and/or poor survival (van ‘t Veer et al., 2002; Minn et al., 2005; Kang et al., 2003; Bos et al., 2009), although the mechanisms orchestrating many of these gene expression programs have not been defined.

The astonishing heterogeneity of tumors (Stephens et al., 2012) also suggests that tumor cells may achieve metastasis through many independent pathways, so the likelihood that targeting a single gene or pathway will prove to be beneficial for many patients is small. On the other hand, if there are coordinated transcriptional programs that drive a significant proportion of metastasis, and, if such programs can be identified in tumors and targeted for therapy, it could advance the field considerably.

It is well established that both genetic and epigenetic events cooperate at all stages of tumor development and progression (Baylin and Jones, 2011). One of the most characteristic epigenetic changes in tumorigenesis is the hypermethylation of CpG islands in promoters of tumor suppressor genes, which is associated with their transcriptional silencing. These methylation changes involve both histone modifications and chromatin remodeling (Suva` et al., 2013).

In addition to epigenetic silencing of specific loci, cancer cell genomes also simultaneously show global DNA hypomethylation (Feinberg and Vogelstein, 1983). This phenomenon leads to abnormal expression of genes and can occur in CpG islands, shores, and large blocks (Hansen et al., 2011; Bert et al., 2013). The cause(s) of global DNA hypomethylation is not understood, nor are the ramifications for tumor progression and metastasis.

Strong evidence has accumulated to support an active DNA demethylation process that involves enzymatic removal of 5-methylcytosine from DNA (Rai et al., 2010; Cortellino et al., 2011; He et al., 2011, Andersen and Jones, 2013). There are several mechanisms now established for active DNA demethylation, so far all of which involve a DNA repair process, but the specific signals that activate the DNA demethylation process remain poorly defined. In particular, how dysfunctional DNA methylation contributes to tumor metastasis is not understood.

RON, also known as macrophage stimulating 1-receptor (MST1R), is a member of the Met family of receptor tyrosine kinases (Ronsin et al., 1993). The biological activity of RON is mediated by binding of its extracellular ligand, macrophage-stimulating protein (MSP), also known as hepatocyte growth factor-like protein (HGFL) and macrophage stimulating 1 (MST1) (Wang et al., 1994; Gaudino et al., 1994). Binding of MSP to its receptor, RON, activates RON and leads to cellular growth, motility, and invasion (Wang et al., 1996; Santoro et al., 1996). Recent studies have documented RON overexpression in a variety of human cancers including those of the breast, colon, liver, pancreas, and bladder, which often correlate with poor outcome (Kretschmann et al., 2010). Moreover, clinical studies have shown that RON overexpression is associated with metastasis and worse patient outcomes. For example, an analysis of microarray gene expression data from 295 breast cancer patients

from the Netherlands Cancer Institute (van de Vijver et al., 2002) revealed that coordinate overexpression of RON, MSP, and MT-SP1 was associated with significantly shorter survival when compared with other patients, indicating that ligand-dependent activation of the RON pathway may promote tumor progression (Welm et al., 2007). Although RON overexpression appears to be a feature of many human cancers, the molecular mechanisms by which RON induces tumorigenesis and metastasis are still unclear.

Here, we show that RON/MSP enhances metastasis of breast cancer xenografts by reprogramming DNA methylation at specific target genes. RON/MSP-initiated differential-DNA methylation is the result of PI3K-dependent upregulation of the methyl-CpG binding domain protein 4 (MBD4), a thymine DNA glycosylase. Knockdown of MBD4 in RON/MSP-expressing breast cancer cells reverses the DNA methylation pattern on specific loci and blocks metastasis. Furthermore, we show that the glycosylase catalytic residue of MBD4 is required for its function in metastasis. We defined a set of genes that are specifically regulated by RON/MSP through MBD4-directed aberrant DNA methylation, and determined that the RON/ MBD4 epigenetic pathway is associated with poor prognosis in breast cancer patients. Importantly, inhibition of Ron signaling with a small molecule kinase inhibitor blocked metastasis of patient-derived tumor grafts, indicating that RON inhibitors may hold promise as antimetastatic agents.

RESULTS

RON/MSP Signaling Promotes Widespread Metastasis of Human Breast Cancer In Vivo

We examined RON expression in six breast epithelial cell lines, including immortalized normal mammary epithelial cells, MCF-10A; two nonmetastatic cancer cell lines, MCF7 and T47D; and three metastatic cancer cell lines, MDA-MB-453, HCC1143, and HCC1806 (Figure 1A). RON was overexpressed in metastatic cancer cell lines compared to normal and nonmetastatic cancer cell lines. To determine whether RON/MSP drives metastasis, we engineered the nonmetastatic MCF7 and T47D breast cancer cell lines to stably express firefly luciferase, and infected them with retroviruses carrying RON and MSP cDNAs (referred to as MCF7-RON/MSP and T47D-RON/MSP; Figure 1A). Over-expressing cells had comparable RON levels with the metastatic breast cancer cell lines.

The effects of RON/MSP gain of function on tumor growth and/or metastasis of MCF7 and T47D tumors were assessed in immune-compromised mice by orthotopic implantation into the cleared inguinal mammary fat pads of 3-week-old female NOD/SCID mice. The growth of tumors was monitored weekly, and tumor metastasis was measured by bioluminescence imaging and histology upon necropsy. The MCF7-RON/MSP cells formed tumors faster compared to parental MCF7 cells, but this was not the case in the T47D model (Figure S1A). To avoid confounding effects of tumor size on metastasis, the mice were euthanized for analysis of metastasis when the tumors reached the same size endpoint for each group. RON/MSP expression was sufficient to induce high rates of spontaneous lung, bone, liver and brain metastasis from MCF7-RON/MSP and T47D-RON/MSP tumors, compared with little or no metastasis from the parental cell xenografts (Figures 1B and 1C). The metastases were verified by histological analysis and immunostaining for human cytokeratin proteins (Figure S1B). These results indicated that RON/MSP expression was sufficient to facilitate

the metastatic spread of MCF7 and T47D breast cancers in vivo to sites that are highly relevant for breast cancer metastasis. These results are consistent with our previous findings, which showed a significant correlation between RON/ MSP expression and metastasis in patients with breast cancer (Welm et al., 2007).

To determine the molecular mechanisms by which RON/ MSP drives breast cancer metastasis, we performed RNA sequencing (RNA-seq) and microarray gene expression profiling of MCF7 and MCF7-RON/MSP cells. Differentially expressed genes (DEGs), based on a false discovery rate threshold of 1% and a fold change of 2, were highly correlated between the two methods. We identified 220 significant DEGs in common with both platforms (Table S1). We used the DAVID bioinformatics database to identify the gene ontology (GO) terms for the DEGs from RNA-seq and micro-array and found significant enrichment for genes involved in plasma membrane, developmental processes, receptor activity and cell signaling/communication. The GO term analysis was not used in our subsequent analysis, but indicated that RON/MSP signaling induces expression of genes whose functions are consistent with biological pathways relevant to metastasis. However, the data did not immediately implicate a clear mechanistic pathway to explain how RON/MSP drives metastasis.

RON/MSP Signaling Upregulates the Thymine Glycosylase MBD4 and Drives Altered DNA Methylation

Regulation of DNA methylation is a major mechanism involved in cell differentiation and neoplastic transformation. The epigenetic modifications contributing to metastasis, however, are much less understood. In order to determine whether alterations in DNA methylation contributed to the selective regulation of RON/MSP-regulated genes, we performed whole-genome bisulfite sequencing (WGBS) on MCF7 and MCF7-RON/MSP cells. We found 1232 differentially-methylated regions (DMRs) (Figure 2A) that occurred in both gene-body and intergenic regions, both inside and outside CpG islands (Figure 2B). DMRs regulated by RON/MSP were often intergenic, and there was a significant enrichment of hypomethylated versus hypermethylated regions (Figures 2A–2C).

Next, we wanted to determine to what degree the DEGs determined by RNA-seq between cell lines were affected by DNA methylation changes. Eleven percent of the DEGs were shown to have significant methylation differences between MCF7 and MCF7-RON/MSP cells. These observations indicated that RON/MSP expression in MCF7 cells induced massive changes in DNA methylation, which also affected expression of particular genes. These data suggested a potential role for altered DNA methylation in the mechanism of RON/MSP-mediated metastasis.

To assess if the aberrant DNA methylation in RON/MSP cells was due to differential expression levels or activities of DNA methyltransferases (DNMTs), we examined mRNA levels of *DNMT3A*, *DNMT3B* and *DNMT1* in MCF7 and MCF7-RON/ MSP cells. We found no statistically significant differences (Figure S2A). We also measured DNMT activity in these cells and found no significant difference between parental cells and those expressing RON/MSP (Figure S2B).

The increased representation of hypomethylated versus hypermethylated DMRs in RON/MSP-expressing cells led us to consider DNA demethylation as a potential effect of RON/MSP. Rai et al. (2008) recently discovered a mechanism for active DNA demethylation in zebrafish that involves the cooperative actions of proteins from the cytidine deaminase family (AID and Apobecs), a G:T mismatch-specific glycosylase (Mbd4) and a DNA repair protein (Gadd45). We examined components of this DNA demethylase complex in MCF7-RON/MSP and T47D-RON/MSP cells. We noted robust upregulation of the thymine DNA glycosylase *MBD4* in cells expressing RON/MSP (Figure 2D). In contrast, another thymine DNA glycosylase (*TDG*), which is implicated in a different mechanism of active DNA demethylation (Cortellino et al., 2011), was not significantly regulated by RON/MSP (Figure 2D). It is also important to note that the TET family, which mediates DNA hydroxymethylation was not regulated by RON/MSP (Figure S2C). Upregulation of MBD4 protein by RON/MSP was validated by western analysis of protein extracts from MCF7 and T47D cell lines (Figure 2E).

To determine whether RON and MBD4 are coordinately expressed in actual human breast tumors, we analyzed *RON* and *MBD4* RNA expression between breast cancer and tumor-adjacent normal samples in the Cancer Genome Atlas (TCGA) data set. *RON* and *MBD4* were both upregulated in breast tumors compared to the normal tissue (Figure 3A). We also examined RON and MBD4 protein expression in three breast reduction tissues and 13 human primary breast tumors by western analysis. RON and MBD4 were highly expressed in all seven poorly differentiated carcinomas. Lower RON and MBD4 levels were found in well-differentiated tumor samples, and little to no MBD4 or RON was detected in control samples taken from breast reduction tissue (Figure 3B). Together with our data showing that MBD4 is expressed downstream of RON/MSP in breast cancer cell lines, these data suggested that RON/MSP might promote aberrant DNA methylation through the up-regulation of MBD4. However, the necessity of MBD4 or DNA methylation for epigenetic regulation of RON/MSP downstream effectors, and any role in metastasis, had never been described.

Knockdown of MBD4 Blocks RON/MSP-Mediated Breast Cancer Metastasis

To investigate the possible role of MBD4 downstream of RON/ MSP in breast cancer metastasis in vivo, MCF7-RON/MSP and T47D-RON/MSP cells were infected with lentiviruses carrying two different MBD4-specific small hairpin RNAs (shRNAs) directed to either the 3’ UTR or the coding region (shMBD4_3UTR and shMBD4_CDS, respectively) or, as controls, anMBD2-specific shRNA (shMBD2) or a scrambled shRNA (shScr). MBD4 knockdown was validated by western blotting (Figure 3C). The effect of MBD4 knockdown on spontaneous metastasis was assessed for both cell lines in NOD/SCID mice. RON/MSP tumors expressing shMBD4 and shScr from both cell lines grew similarly to the tumors derived from RON/MSP cells; therefore, MBD4 loss of function had no effect on primary tumor growth (Figure S3A). However, spontaneous lung, liver, bone and brain metastasis was significantly inhibited in animals carrying MCF7-RON/MSP-shMBD4 and T47D-RON/MSP-shMBD4 tumors relative to the control tumors expressing RON/MSP (Figures 3D and 3E). In fact, metastasis frequencies of RON/MSP-shMBD4 cells were not significantly different from the original parental cell lines, approaching 0%. The RON/MSP-shMBD2 and

the RON/MSP-shScr control tumors showed a similar frequency of metastasis as the RON/MSP tumors (Figures 3D, 3E, S3B, and S3C). To rule out off-target effects of the MBD4 shRNAs, we generated MBD4 cDNA rescue constructs (MBD4R-3UTR and MBD4R-CDS) that were resistant to their respective shRNAs. We then conducted rescue experiments in MCF7-RON/MSP-shMBD4 and T47D-RON/MSP-shMBD4 cells where re-expression ofMBD4 was at similar levels to that found in RON/MSP cells (Figure 3C). Expression of MBD4R reversed the inhibition of RON/MSP-mediated metastasis by shMBD4 (Figures 3D and 3E). These data confirm that RON/MSP drives metastasis through upregulation of MBD4, at least in these two models.

To determine whether MBD4 requires its glycosylase activity to drive metastasis, we engineered an MBD4 rescue cDNA containing a single amino acid mutation of the catalytic residue, D560A. This mutant has previously been shown to be catalytically dead (Hendrich et al., 1999, Petronzelli et al., 2000). We transplanted MCF7 and T47D cells expressing RON/MSP-shMBD4R (D560A) into mammary fad pads of NOD/SCID mice and monitored metastasis. The mutation prevented the rescue of the metastasis phenotype observed with the wild-type MBD4 rescue constructs, suggesting that MBD4 is driving metastasis through its glycosylase activity (Figures 3D and 3E). We next sought to determine if MBD4 was also required for reprogramming of DNA methylation downstream of RON/MSP.

Knockdown of MBD4 Reverses Abnormal DNA Methylation Patterns and Reverses Expression of RON/MSP-Regulated Genes

To investigate the requirement for MBD4 in aberrant DNA methylation driven by RON/MSP, we analyzed WGBS data from MCF7-RON/MSP-shMBD4 compared to MCF7-RON/MSP. MBD4 knockdown reversed the methylation status of a specific collection of loci in MCF7-RON/MSP cells. These regions of aberrant DNA methylation were reprogrammed following the knockdown of MBD4, to levels that were comparable with parental MCF7 cells (Figures 4A and 4B). It is important to note that knocking down MBD4 also caused changes in methylation of some loci that were independent of RON/MSP (Figure 4C).

To further understand the role of MBD4-mediated aberrant DNA methylation in gene expression downstream of RON/ MSP, we also performed RNA-sequencing and microarray gene expression profiling of MCF7-RON/MSP-shMBD4 cells. We found that a statistically significant 25% of genes that were regulated by RON/MSP in MCF7 cells became reversed by MBD4 knockdown (Figure 4D). Reversal of this gene expression pattern correlated with lack of metastasis upon MBD4 knockdown. It is important to note that there were other gene expression changes induced by RON/MSP that were independent of MBD4 and vice versa. Thus, as expected, RON signaling does contribute other changes to cancer cells. Likewise, knockdown of MBD4 also affected expression of genes other than those regulated by RON/MSP, suggesting that MBD4 can also regulate expression of genes outside of the RON/MSP pathway. To dissect specific effects of the RON/MSP-MBD4 pathway, we focused on the gene set that was both RON/MSP-dependent and MBD4-dependent (reversed in RON/MSP cells when MBD4 was knocked down).

Using our WGBS and RNaseq data, we identified all of the genes that were regulated by RON/MSP in MCF7 cells that were also reversed by MBD4 knockdown. We identified 192

genes (Figure 5A), of which 64 were differentially methylated at the same locus. Because we could not definitively determine whether the remaining 128 genes were also regulated by DNA methylation in a distant region (e.g., enhancer region or inter-chromosomal interacting regions) (Bert et al., 2013, Hsu et al., 2013), we grouped all 192 RON/MBD4-dependent DEGs collectively and refer to them as the “RON/MBD4 epigenetic signature” (Figure 5A).

Specific Subclasses of Human Breast Tumors Possess the RON/MBD4 Epigenetic Signature, which Correlates with Poor Prognosis

Although experimentation on human cancer cell lines is essential for dissection of mechanistic pathways in cancer biology, it is an extrapolation from bona fide tumors. Therefore, we asked whether the RON/MBD4 epigenetic reprogramming pathway that we identified and functionally characterized in cell line models exists in human breast tumors and, if so, whether it is associated with survival outcome. To first determine whether the RON/MBD4 epigenetic signature is present in human breast tumors, we used a gene module map (Segal et al., 2004) to examine the expression of 116 genes of the 192 above-mentioned genes in 997 primary human breast cancers from the Metabric discovery cohort (the remainder of the genes were not annotated in the Metabric data set; Curtis et al., 2012). The RON/MBD4 epigenetic metastasis signature was present approximately in 25% of the breast cancers (Figure 5B).

Using the published clinical annotations for each tumor (tumor grade, expression of estrogen and progesterone receptors (ER/ PR), and HER2 status), we found that the RON/MBD4 epigenetic signature was significantly associated with grade 3, ER, and PR, tumors (Figure 5B). Several “intrinsic subtypes” of breast cancer have been previously defined on the basis of more comprehensive gene expression profiles: normal-like, luminal type A, luminal type B, HER2 like, and basal like (Sørlie et al., 2001). Indeed, the RON/MBD4 epigenetic signature was significantly enriched in basal-like tumors (Figure 5B).

We next performed Kaplan-Meier analysis examining overall survival for individuals with breast cancer across the 997 patient METABRIC data set, using the annotated 116 gene RON/MBD4 epigenetic signature. The expression of these genes was significantly associated with poor survival ($p < 0.05$, hazard ratio [HR] = 1.30, Figure 5C). These data strongly suggest that the RON/MBD4 pathway exists in a fairly large subset of human breast cancers (25%), and that detection of the RON/MBD4 epigenetic pathway may significantly contribute to risk assessment in breast cancer patients, even though the signature was generated a priori from all genes in the RON/MBD4 pathway. An important corollary to this work was to next ask how RON regulates MBD4 and whether the presence of a RON/MBD4 epigenetic signature would predict response to anti-Ron therapy.

MBD4 Is Upregulated by RON/MSP through PI3K Signaling

In order to further characterize MBD4 regulation by RON, we engineered an MCF7-TRE-RON/MSCV-tTA cell line, where RON expression is under the control of the tetracycline (Tet) response element (TRE) and is repressed by binding of doxycycline (dox) to the Tet transactivator protein (tTA). As expected, in the absence of dox the cells expressed RON, which began to be repressed 4 hr after the addition of dox to the culture medium and was

maximally repressed 48 hr after adding dox (Figure 6A). Consistent with data in Figures 2D and 2E showing that RON regulates MBD4, we found that repression of RON also causes downregulation of MBD4 (Figure 6A). To determine whether repression of endogenous RON causes downregulation of MBD4 in other model systems, RON was knocked down using shRNA via lentiviral infection in both the RON-positive DU4475 breast cancer cell line and in primary culture from a RON-positive patient-derived breast tumor graft (DeRose et al., 2011). Scrambled shRNA was used as control. RON knockdown, although not complete, caused a reduction in MBD4 expression in both models (Figure 6B). Thus, we concluded that, in all five different models we examined, RON upregulates MBD4, which can be reversed with RON downregulation. Therefore, the pathway has potential to be blocked.

RON is known to transduce a variety of signals that regulate different downstream pathways, most notably the mitogen-activated protein kinase (MAPK) and phosphatidylinositol 3-kinase (PI3K) pathways (Li et al., 1995; Wang et al., 1996). To elucidate which signaling pathway(s) is required for regulation of MBD4 by RON, we treated the cell lines with varying doses of U0126 (a MEK/ERK inhibitor), or BKM-120 (a PI3K inhibitor) for 0.5 hr or 1 hr, followed by protein extraction and MBD4 western blotting. Examination of activated (phosphorylated) Erk and PRAS proteins in each experiment verified that the drugs were effective in inhibiting their respective targets (Figure 6C). Treatment with BKM-120, but not U0126, blocked RON/MSP-mediated MBD4 upregulation (Figure 6C). To further validate that MBD4 upregulation by RON/MSP requires PI3K/Akt signaling, the PI3K p110 alpha catalytic subunit was knocked down in MCF7-RON/MSP cells by shRNA via lentiviral infection. Knockdown of PI3K activity was determined using phosphorylation of PRAS as a surrogate measure (Figure 6D). This experiment showed that PI3K knockdown led to a reduction in MBD4 expression, similar to the results with BKM-120 (Figure 6C), demonstrating that RON/MSP regulates MBD4 through activation of the PI3K pathway.

To determine whether MBD4 is regulated specifically by RON/ MSP-mediated activation of PI3K, we engineered MCF7 cells to overexpress the other member of the MET receptor tyrosine kinase family, MET, which also activated PI3K (Figure S4A). We found that MET increased MBD4 expression, showing that MBD4 can be regulated by another, related tyrosine kinase (Figure S4A). To determine whether any activator of PI3K signaling could increase MBD4 expression, we treated EGFR-positive MDA-MB-231 cells with EGF (15 nM) for 30 min, which was sufficient to activate PI3K as determined by phosphorylation of AKT (Figure S4B). We observed no upregulation of MBD4, indicating that MBD4 is not universally regulated by activation of the PI3K pathway (Figure S4B). It is also important to note that MBD4 phosphorylation was not altered as a result of RON/MSP pathway activation (Figure S4C), suggesting that MBD4 is not a direct target of RON kinase or kinases in the PI3K pathway.

Treatment with a RON Kinase Inhibitor Prevents Metastasis of Primary Patient-Derived Tumor Grafts

Ron kinase activity, and its resulting signaling, can be blocked by small molecule kinase inhibitors. To determine if the RON/ MBD4 pathway can be blocked in patient tumors using

RON kinase inhibitors, and if there is a resulting effect on metastasis, we utilized four independent experimental systems that are highly relevant to bona fide breast tumors. First, we chose two patient-derived tumor grafts (DeRose et al., 2011) that survive primary culture conditions and treated them with the RON/ MET dual inhibitor OSI-296 (Steinig et al., 2013) in vitro. Inhibition of RON (verified by reduction of phosphorylated RON protein) caused downregulation of MBD4 (Figure 7A). Next, we chose two human tumor graft lines for in vivo studies based on their RON/MBD4 signature (not shown) and on their relatively fast growth and robust metastasis (DeRose et al., 2011), which allows for assessment of tumor growth and metastasis within a timeline that is practical for drug treatment. The tumor grafts were implanted orthotopically into cleared mammary fat pads of NOD/SCID mice and allowed to grow to 100 mm^3 before starting treatment with OSI-296. Although there was no significant effect on tumor growth (data not shown), inhibition of RON in the in vivo setting caused complete blockade of lymph node (Figures 7B and 7C) and lung (Figure 7D) metastasis in these two models.

To determine whether the RON/MBD4 pathway that we previously defined in MCF7 cells was affected in the tumor grafts treated with the Ron kinase inhibitor in vivo, we analyzed gene expression in tumors from mice treated with the vehicle (Trappsol) or OSI-296. Indeed, a set of nine genes (*CSGALNACT1*, *SIGLEC6*, *SHC4*, *ABCA1*, *PLD1*, *RNF144A*, *SLC44A4*, *SLC2A13*, and *AXIN2*) from the RON/ MBD4 epigenetic signature was significantly deregulated following treatment with the RON inhibitor in vivo. These data indicated that short-term inhibition of RON kinase with OSI-296 could not only block metastasis, but also reverse expression of some genes within the RON/MBD4 epigenetic metastasis signature.

To assess whether the expression of these nine RON/MBD4-dependent genes was associated with patient outcome in breast cancer cohorts, we performed Kaplan-Meier analysis examining overall survival for individuals with breast cancer across the 997 patient METABRIC data set (Curtis et al., 2012). The expression of these nine genes (defined as the subset of the RON/MBD4 epigenetic signature genes that were reversed in tumor grafts following RON inhibitor treatment) was significantly associated with poor survival ($p = 0.04$, HR = 1.55, Figure 7E). To validate our findings using additional, independent data, we generated a meta collection of gene expression data from an additional 977 patients from five independently published studies of breast cancer (van ‘t Veer et al., 2002; Miller et al., 2005; Chin et al., 2006; Desmedt et al., 2007; Heikkinen et al., 2011). The method we utilized to normalize data across the different data sets was previously described (Segal et al., 2004; Ben-Porath et al., 2008). Using these data, we confirmed that the nine gene RON/ MBD4 epigenetic signature was significantly associated with poor survival ($p = 0.008$, HR = 1.55, Figure 7E).

Interestingly, multivariate analysis of the nine gene RON/ MBD4 epigenetic signature revealed that it was not a significant independent prognostic factor for survival in this data set and may depict similar risk as ER− status (Figure 7F). ER− tumors have a poor prognosis, in part because there are no targeted therapy options due to lack of defined pathways driving these tumors. Together, these data highlight the promising potential for (1) identifying breast cancer patients that might benefit from a RON inhibitor (approximately

25%); (2) identifying a set of biomarkers for RON inhibition, and (3) blocking RON to inhibit breast cancer metastasis.

DISCUSSION

Although more than 90% of cancer mortality is attributable to metastasis, the requisite events for this complicated process are still largely unknown. Our ability to treat metastatic disease, or to better treat those at high risk for metastatic disease in the adjuvant setting, effectively depends on our ability to block or reverse the progression of metastases. We have identified an epigenetic pathway downstream of RON/PI3K signaling that drives a key metastatic program for breast cancer. Human breast cancers can be stratified by the presence or absence of this program, which provides significant prognostic information for risk of metastatic relapse. Moreover, treatment of mice with a RON inhibitor blocked metastasis of aggressive patient-derived tumor grafts. These data provide several important insights, given that a specific event leading to reprogramming of DNA methylation has not previously been implicated in metastasis and that RON is not known to regulate any aspect of epigenetic reprogramming.

Our data also indicated that the RON/MBD4 methylation program may be a prognostic biomarker for patient outcome, and potentially may be used to predict response to RON inhibitors. Although the effect on hazard ratio with either signature (116 or 9 genes) in the large patient cohorts we examined is somewhat modest, it is consistent with our appreciation for breast tumor heterogeneity. Outcomes from the TCGA project in breast cancer revealed very few high-frequency alterations (Stephens et al., 2012). Therefore, due to intertumor heterogeneity, small subsets of patients will need to be preselected in order to detect significant therapeutic effects, even with drugs that are potentially very effective for particular subsets of patients. Our data suggest a way to select populations of breast cancer patients that might benefit from RON inhibitor therapy.

Receptor tyrosine kinase signaling has been shown to be involved in promoting aggressive tumor phenotypes and has provided a rich source of drug targets (Krause and Van Etten, 2005). Here, we show that RON/MSP functions through PI3K signaling to induce expression of the DNA glycosylase MBD4. Once upregulated, MBD4 induces epigenetic reprogramming of breast cancer cells, which drives metastasis in a glycosylase-dependent manner. Importantly, metastasis can be inhibited by MBD4 knockdown, which reverses the DNA methylation status of a specific collection of loci in MCF7-RON/ MSP cells. MBD4 knockdown also leads to reversal in expression of 192 RON/MSP target genes. MBD4 expression can be downregulated by blocking RON kinase activity or PI3K activity, indicating that blocking the metastatic program that we have described here is clinically feasible. PI3K inhibitors are currently in clinical trials for several cancers, and RON inhibitors are in early stage trials with multiple compounds in clinical development.

One important issue with regard to RON kinase inhibitors is that the RON and MET kinase domains are 68% identical. Most RON-selective, ATP-competitive small molecules inhibit both RON and MET, and vice versa. However, targeting the kinase activity of RON is predicted be more effective than the more specific ligand-blocking antibody approaches

because several different isoforms of RON exist, including ligand-independent constitutively active forms (Liu et al., 2011; Wang et al., 2010). Therefore, the most effective RON inhibitors may also inhibit MET, at least to some degree. In elucidating the RON/MBD4 epigenetic reprogramming pathway described here, we started with a gain-of-function model using RON/ MSP overexpression and then validated the results using a loss-of-function (RON-specific shRNA) approach, so we are confident that regulation of MBD4 is truly a function of RON. Likewise, the RON inhibitors that we used phenocopied the RON shRNA data, indicating that RON was the effective target. In the clinical situation, dual inhibition of RON and MET may actually be beneficial to cancer patients because both proteins can drive aggressive phenotypes (albeit usually in different cancers), and because MET-selective inhibitors that also inhibit RON have not shown profound toxicity in clinical trials.

DNA methylation and other epigenetic alterations have been previously associated with metastasis, especially at the single gene level (Feng et al., 2010; Chen et al., 2009; Han et al., 2008). More recently, genome-wide DNA methylation patterns have been described in breast cancer metastasis (Fang et al., 2011; Rodenhiser et al., 2008); however, the mechanism(s) driving altered DNA methylation in metastasis have not been described. This study shows a specific pathway that drives epigenetic reprogramming to facilitate metastasis.

Future studies will be required to address how aberrant DNA methylation is targeted to particular loci in RON/MSP-expressing tumors; which aberrant regulated loci (or combinations of loci) give rise to a metastatic phenotype; and how these RON/MBD4 target genes promote metastasis. In addition to the targeted DNA methylation changes at specific loci, factors such as nuclear organization, chromatin remodeling, and histone modifications may impart profound changes in genome-wide methylation patterns (Jones, 2012). Thus, aberrant DNA methylation downstream of RON/MSP may involve a variety of mechanisms, all of which may serve to promote and/or sustain metastasis. Just as tumor cells presumably need to simultaneously regulate cohorts of genes to achieve the complex process of metastasis, clinical treatments to prevent metastasis may have to inhibit multiple pathways simultaneously. Thus, reversing the epigenetic reprogramming events revealed here may provide a more effective approach to cancer treatment.

EXPERIMENTAL PROCEDURES

In Vivo Metastasis

All animal procedures were reviewed and approved by the University of Utah Institutional Animal Care and Use Committee. For bioluminescence imaging, mice were anesthetized and given 150 mg/kg of D-luciferin in PBS by i.p. injection. Five minutes after injection, mice were killed and the organs were extracted and imaged ex vivo to detect metastasis foci. A detailed description of analysis is provided in Supplemental Experimental Procedures.

Expression Array Hybridization and Data Analysis

Triplicate biological replicates of hybridization were performed for each cell line. Differential gene expression was evaluated using the t test ($p < 0.01$) and Benjamini and Hochberg correction. The threshold was set at 2-fold change for both upregulated and

downregulated genes. A detailed description of analysis is provided in Supplemental Experimental Procedures.

RNA Sequencing

Alignments were generated from Illumina Fastq files to the hg19 human genome with all known and theoretical splice junctions using Novocraft's novoalign aligner. A detailed description of analysis is provided in Supplemental Experimental Procedures.

Computational Analytical Method for WGBS

The software packages used in this analysis are open source and available from the USeq (http://useq.sourceforge.net/usageBisSeq.html) project website (Nix et al., 2010). A detailed description of analysis is provided in Supplemental Experimental Procedures.

Analysis of Gene-Set Enrichment Patterns

To identify gene-set enrichment patterns, we used methods described previously (Segal et al., 2004) applied with Genomica. A detailed description of analysis is provided in Supplemental Experimental Procedures.

Survival Analysis

All survival data were extracted from original publications. p values were calculated using the log rank test comparing the group of individuals with tumors showing the RON/MBD4 signature to all other individuals. Univariate and multivariate analyses with Cox proportional-hazards regression were done on the individual clinical variables.

Supplementary Material

Refer to Web version on PubMed Central for supplementary material.

Acknowledgments

This work was funded by the DOD Breast Cancer Research Program Era of Hope Scholar Award (to A.L.W.), a Susan G. Komen for the Cure Career Catalyst Award (to A.L.W.), and the Huntsman Cancer Institute and Foundation. We utilized the Cancer Center's Microarray and Genomic Analysis Shared Resource, the Comparative Oncology Resource, and the University of Utah Health Sciences Center Bioinformatics and DNA Sequencing core facilities. We thank members of Dr. David Jones' and Dr. Bradley Cairns' labs for useful input and for critical reading of the manuscript. We thank Brian Dalley for help with genomics, and Darren Ames, David Nix, and Brett Milash for assistance with computational data analysis. This study makes use of data generated by the Molecular Taxonomy of Breast Cancer International Consortium. Funding for that project was provided by Cancer Research UK and the British Columbia Cancer Agency Branch. M.R.A., S.T., and M.J.M. are former employees of OSI/Astellas and hold stock in this company. A.L.W. received funding from OSI/Astellas to support work investigating RON inhibitors.

REFERENCES

Andersen A, Jones DA. APC and DNA demethylation in cell fate specification and intestinal cancer. Adv. Exp. Med. Biol. 2013; 754:167–177. [PubMed: 22956501]

Baylin SB, Jones PA. A decade of exploring the cancer epigenome - biological and translational implications. Nat. Rev. Cancer. 2011; 11:726–734. [PubMed: 21941284]

Ben-Porath I, Thomson MW, Carey VJ, Ge R, Bell GW, Regev A, Weinberg RA. An embryonic stem cell-like gene expression signature in poorly differentiated aggressive human tumors. Nat. Genet. 2008; 40:499–507. [PubMed: 18443585]

Bert SA, Robinson MD, Strbenac D, Statham AL, Song JZ, Hulf T, Sutherland RL, Coolen MW, Stirzaker C, Clark SJ. Regional activation of the cancer genome by long-range epigenetic remodeling. Cancer Cell. 2013; 23:9–22. [PubMed: 23245995]

Bos PD, Zhang XH, Nadal C, Shu W, Gomis RR, Nguyen DX, Minn AJ, van de Vijver MJ, Gerald WL, Foekens JA, Massagué J. Genes that mediate breast cancer metastasis to the brain. Nature. 2009; 459:1005–1009. [PubMed: 19421193]

Chen SS, Raval A, Johnson AJ, Hertlein E, Liu TH, Jin VX, Sherman MH, Liu SJ, Dawson DW, Williams KE, et al. Epigenetic changes during disease progression in a murine model of human chronic lymphocytic leukemia. Proc. Natl. Acad. Sci. USA. 2009; 106:13433–13438. [PubMed: 19666576]

Chin K, DeVries S, Fridlyand J, Spellman PT, Roydasgupta R, Kuo WL, Lapuk A, Neve RM, Qian Z, Ryder T, et al. Genomic and transcriptional aberrations linked to breast cancer pathophysiologies. Cancer Cell. 2006; 10:529–541. [PubMed: 17157792]

Cortellino S, Xu J, Sannai M, Moore R, Caretti E, Cigliano A, Le Coz M, Devarajan K, Wessels A, Soprano D, et al. Thymine DNA glycosylase is essential for active DNA demethylation by linked deamination-base excision repair. Cell. 2011; 146:67–79. [PubMed: 21722948]

Curtis C, Shah SP, Chin SF, Turashvili G, Rueda OM, Dunning MJ, Speed D, Lynch AG, Samarajiwa S, Yuan Y, et al. METABRIC Group. The genomic and transcriptomic architecture of 2,000 breast tumours reveals novel subgroups. Nature. 2012; 486:346–352. [PubMed: 22522925]

DeRose YS, Wang G, Lin YC, Bernard PS, Buys SS, Ebbert MT, Factor R, Matsen C, Milash BA, Nelson E, et al. Tumor grafts derived from women with breast cancer authentically reflect tumor pathology, growth, metastasis and disease outcomes. Nat. Med. 2011; 17:1514–1520. [PubMed: 22019887]

Desmedt C, Piette F, Loi S, Wang Y, Lallemand F, Haibe-Kains B, Viale G, Delorenzi M, Zhang Y, d'Assignies MS, et al. TRANSBIG Consortium. Strong time dependence of the 76-gene prognostic signature for node-negative breast cancer patients in the TRANSBIG multicenter independent validation series. Clin. Cancer Res. 2007; 13:3207–3214. [PubMed: 17545524]

Fang F, Turcan S, Rimner A, Kaufman A, Giri D, Morris LG, Shen R, Seshan V, Mo Q, Heguy A, et al. Breast cancer methylomes establish an epigenomic foundation for metastasis. Sci. Transl. Med. 2011; 3:75ra25.

Feinberg AP, Vogelstein B. Hypomethylation distinguishes genes of some human cancers from their normal counterparts. Nature. 1983; 301:89–92. [PubMed: 6185846]

Feng W, Orlandi R, Zhao N, Carcangiu ML, Tagliabue E, Xu J, Bast RC Jr, Yu Y. Tumor suppressor genes are frequently methylated in lymph node metastases of breast cancers. BMC Cancer. 2010; 10:378. [PubMed: 20642860]

Gaudino G, Follenzi A, Naldini L, Collesi C, Santoro M, Gallo KA, Godowski PJ, Comoglio PM. RON is a heterodimeric tyrosine kinase receptor activated by the HGF homologue MSP. EMBO J. 1994; 13:3524–3532. [PubMed: 8062829]

Han HJ, Russo J, Kohwi Y, Kohwi-Shigematsu T. SATB1 reprogrammes gene expression to promote breast tumour growth and metastasis. Nature. 2008; 452:187–193. [PubMed: 18337816]

Hansen KD, Timp W, Bravo HC, Sabunciyan S, Langmead B, McDonald OG, Wen B, Wu H, Liu Y, Diep D, et al. Increased methylation variation in epigenetic domains across cancer types. Nat. Genet. 2011; 43:768–775. [PubMed: 21706001]

He YF, Li BZ, Li Z, Liu P, Wang Y, Tang Q, Ding J, Jia Y, Chen Z, Li L, et al. Tet-mediated formation of 5-carboxylcytosine and its excision by TDG in mammalian DNA. Science. 2011; 333:1303–1307. [PubMed: 21817016]

Heikkinen T, Greco D, Pelttari LM, Tommiska J, Vahteristo P, Heikkilä P, Blomqvist C, Aittomäki K, Nevanlinna H. Variants on the promoter region ofPTEN affect breastcancer progression and patient survival. Breast Cancer Res. 2011; 13:R130. [PubMed: 22171747]

Hendrich B, Hardeland U, Ng HH, Jiricny J, Bird A. The thymine glycosylase MBD4 can bind to the product of deamination at methylated CpG sites. Nature. 1999; 401:301–304. [PubMed: 10499592]

Hsu PY, Hsu HK, Lan X, Juan L, Yan PS, Labanowska J, Heerema N, Hsiao TH, Chiu YC, Chen Y, et al. Amplification of distant estrogen response elements deregulates target genes associated with tamox-ifen resistance in breast cancer. Cancer Cell. 2013; 24:197–212. [PubMed: 23948299]

Jones PA. Functions of DNA methylation: islands, start sites, gene bodies and beyond. Nat. Rev. Genet. 2012; 13:484–492. [PubMed: 22641018]

Kang Y, Siegel PM, Shu W, Drobnjak M, Kakonen SM, Cordón-Cardo C, Guise TA, Massagué J. A multigenic program mediating breast cancer metastasis to bone. Cancer Cell. 2003; 3:537–549. [PubMed: 12842083]

Krause DS, Van Etten RA. Tyrosine kinases as targets for cancer therapy. N. Engl. J. Med. 2005; 353:172–187. [PubMed: 16014887]

Kretschmann KL, Eyob H, Buys SS, Welm AL. The macro-phage stimulating protein/Ron pathway as a potential therapeutic target to impede multiple mechanisms involved in breast cancer progression. Curr. Drug Targets. 2010; 11:1157–1168. [PubMed: 20545605]

Krzywinski M, Schein J, Birol I, Connors J, Gascoyne R, Horsman D, Jones SJ, Marra MA. Circos: an information aesthetic for comparative genomics. Genome Res. 2009; 19:1639–1645. [PubMed: 19541911]

Li BQ, Wang MH, Kung HF, Ronsin C, Breathnach R, Leonard EJ, Kamata T. Macrophage-stimulating protein activates Ras by both activation and translocation of SOS nucleotide exchange factor. Biochem. Biophys. Res. Commun. 1995; 216:110–118. [PubMed: 7488076]

Liu X, Zhao L, Derose YS, Lin YC, Bieniasz M, Eyob H, Buys SS, Neumayer L, Welm AL. Short-form Ron promotes spontaneous breast cancer metastasis through interaction with phosphoinositide 3-kinase. Genes Cancer. 2011; 2:753–762. [PubMed: 22207901]

Miller LD, Smeds J, George J, Vega VB, Vergara L, Ploner A, Pawitan Y, Hall P, Klaar S, Liu ET, Bergh J. An expression signature for p53 status in human breast cancer predicts mutation status, transcriptional effects, and patient survival. Proc. Natl. Acad. Sci. USA. 2005; 102:13550–13555. [PubMed: 16141321]

Minn AJ, Gupta GP, Siegel PM, Bos PD, Shu W, Giri DD, Viale A, Olshen AB, Gerald WL, Massagué J. Genes that mediate breast cancer metastasis to lung. Nature. 2005; 436:518–524. [PubMed: 16049480]

Nix DA, Di Sera TL, Dalley BK, Milash BA, Cundick RM, Quinn KS, Courdy SJ. Next generation tools for genomic data generation, distribution, and visualization. BMC Bioinformatics. 2010; 11:455. [PubMed: 20828407]

Petronzelli F, Riccio A, Markham GD, Seeholzer SH, Stoerker J, Genuardi M, Yeung AT, Matsumoto Y, Bellacosa A. Biphasic kinetics of the human DNA repair protein MED1 (MBD4), a mismatch-specific DNA N-glycosylase. J. Biol. Chem. 2000; 275:32422–32429. [PubMed: 10930409]

Rai K, Huggins IJ, James SR, Karpf AR, Jones DA, Cairns BR. DNA demethylation in zebrafish involves the coupling of a deaminase, a glycosylase, and gadd45. Cell. 2008; 135:1201–1212. [PubMed: 19109892]

Rai K, Sarkar S, Broadbent TJ, Voas M, Grossmann KF, Nadauld LD, Dehghanizadeh S, Hagos FT, Li Y, Toth RK, et al. DNA demethylase activity maintains intestinal cells in an undifferentiated state following loss of APC. Cell. 2010; 142:930–942. [PubMed: 20850014]

Rodenhiser DI, Andrews J, Kennette W, Sadikovic B, Mendlowitz A, Tuck AB, Chambers AF. Epigenetic mapping and functional analysis in a breast cancer metastasis model using whole-genome promoter tiling microarrays. Breast Cancer Res. 2008; 10:R62. [PubMed: 18638373]

Ronsin C, Muscatelli F, Mattei MG, Breathnach R. A novel putative receptor protein tyrosine kinase of the met family. Oncogene. 1993; 8:1195–1202. [PubMed: 8386824]

Santoro MM, Collesi C, Grisendi S, Gaudino G, Comoglio PM. Constitutive activation of the RON gene promotes invasive growth but not transformation. Mol. Cell. Biol. 1996; 16:7072–7083. [PubMed: 8943362]

Segal E, Friedman N, Koller D, Regev A. A module map showing conditional activity of expression modules in cancer. Nat. Genet. 2004; 36:1090–1098. [PubMed: 15448693]

Sørlie T, Perou CM, Tibshirani R, Aas T, Geisler S, Johnsen H, Hastie T, Eisen MB, van de Rijn M, Jeffrey SS, et al. Gene expression patterns of breast carcinomas distinguish tumor subclasses with clinical implications. Proc. Natl. Acad. Sci. USA. 2001; 98:10869–10874. [PubMed: 11553815]

Steinig AG, Li AH, Wang J, Chen X, Dong H, Ferraro C, Jin M, Kadal-bajoo M, Kleinberg A, Stolz KM, et al. Novel 6-aminofuro[3,2-c]pyridines as potent, orally efficacious inhibitors of cMET and RON kinases. Bioorg. Med. Chem. Lett. 2013; 23:4381–4387. [PubMed: 23773865]

Stephens PJ, Tarpey PS, Davies H, Van Loo P, Greenman C, Wedge DC, Nik-Zainal S, Martin S, Varela I, Bignell GR, et al. Oslo Breast Cancer Consortium (OSBREAC). The landscape of cancer genes and mutational processes in breast cancer. Nature. 2012; 486:400–404. [PubMed: 22722201]

Suvà ML, Riggi N, Bernstein BE. Epigenetic reprogramming in cancer. Science. 2013; 339:1567–1570. [PubMed: 23539597]

van de Vijver MJ, He YD, van't Veer LJ, Dai H, Hart AA, Voskuil DW, Schreiber GJ, Peterse JL, Roberts C, Marton MJ, et al. A gene-expression signature as a predictor of survival in breast cancer. N. Engl. J. Med. 2002; 347:1999–2009. [PubMed: 12490681]

van 't Veer LJ, Dai H, van de Vijver MJ, He YD, Hart AA, Mao M, Peterse HL, van der Kooy K, Marton MJ, Witteveen AT, et al. Gene expression profiling predicts clinical outcome of breast cancer. Nature. 2002; 415:530–536. [PubMed: 11823860]

Wang MH, Ronsin C, Gesnel MC, Coupey L, Skeel A, Leonard EJ, Breathnach R. Identification of the ron gene product as the receptor for the human macrophage stimulating protein. Science. 1994; 266:117–119. [PubMed: 7939629]

Wang MH, Montero-Julian FA, Dauny I, Leonard EJ. Requirement of phosphatidylinositol-3 kinase for epithelial cell migration activated by human macrophage stimulating protein. Oncogene. 1996; 13:2167–2175. [PubMed: 8950984]

Wang MH, Padhye SS, Guin S, Ma Q, Zhou YQ. Potential therapeutics specific to c-MET/RON receptor tyrosine kinases for molecular targeting in cancer therapy . Acta Pharmacol. Sin. 2010; 31:1181–1188. [PubMed: 20694025]

Welm AL, Sneddon JB, Taylor C, Nuyten DS, van de Vijver MJ, Hase-gawa BH, Bishop JM. The macrophage-stimulating protein pathway promotes metastasis in a mouse model for breast cancer and predicts poor prognosis in humans. Proc. Natl. Acad. Sci. USA. 2007; 104:7570–7575. [PubMed: 17456594]

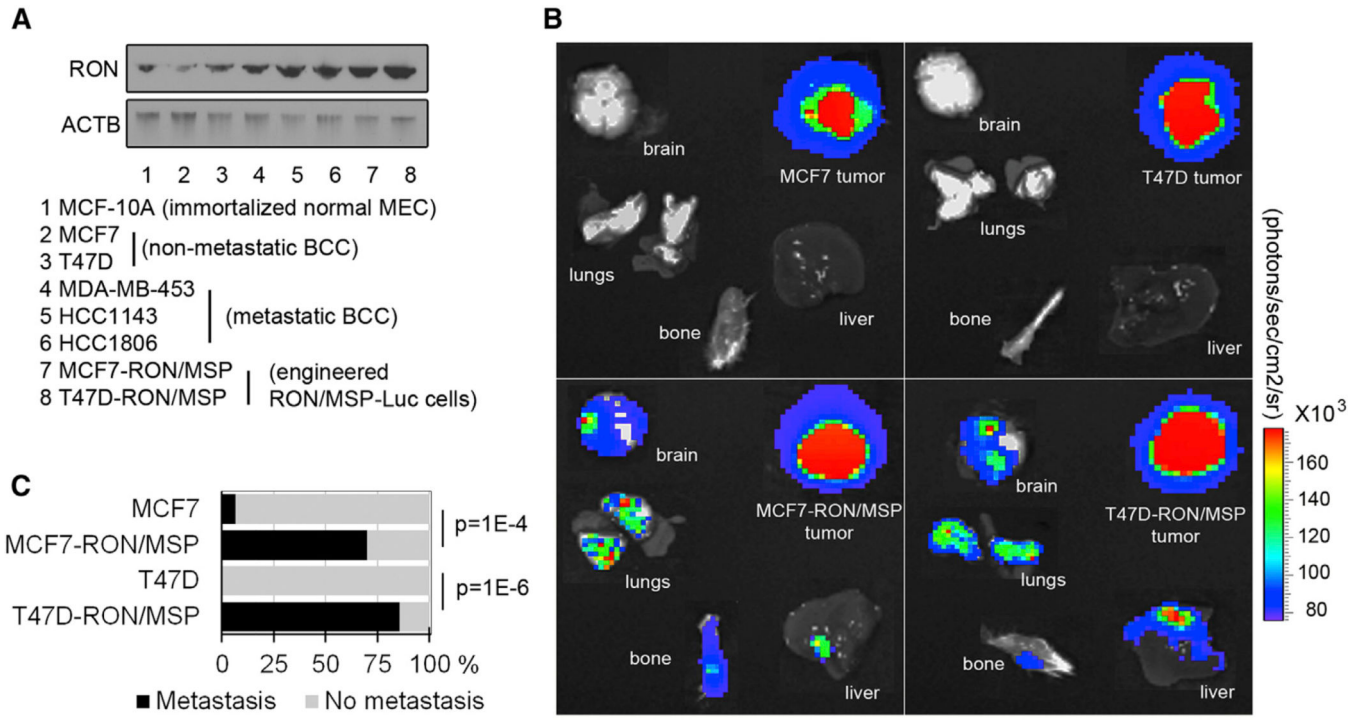

Figure 1. RON/MSP Signaling Promotes Widespread Metastasis of Human Breast Cancer In Vivo

(A) Immunoblot analysis of RON levels (top) in immortalized mammary epithelial cells (MCF-10A), nonaggressive breast cancer cell lines (MCF7 and T47D), aggressive breast cancer cell lines (MDA-MB-453, HCC1143, HCC1806), and MCF7 and T47D cells engineered to overexpress RON/MSP. The β-actin (ACTB) loading control is shown in the bottom panel.

(B) The effect of RON/MSP on spontaneous lung, bone, liver, and brain metastasis of orthotopic MCF7 and T47D tumors. Shown are representative bioluminescent images of primary tumors, lung, bone, liver, and brain metastasis from single mice.

(C) Metastasis frequencies for MCF7 (n = 15), MCF7-RON/MSP (n = 20), T47D (n = 16), and T47D-RON/MSP (n = 14) tumors following orthotopic injection into mammary fat pad of NOD/SCID mice. All RON/MSP tumors were harvested when size-matched to parental tumors.

See also Figure S1 and Table S1.

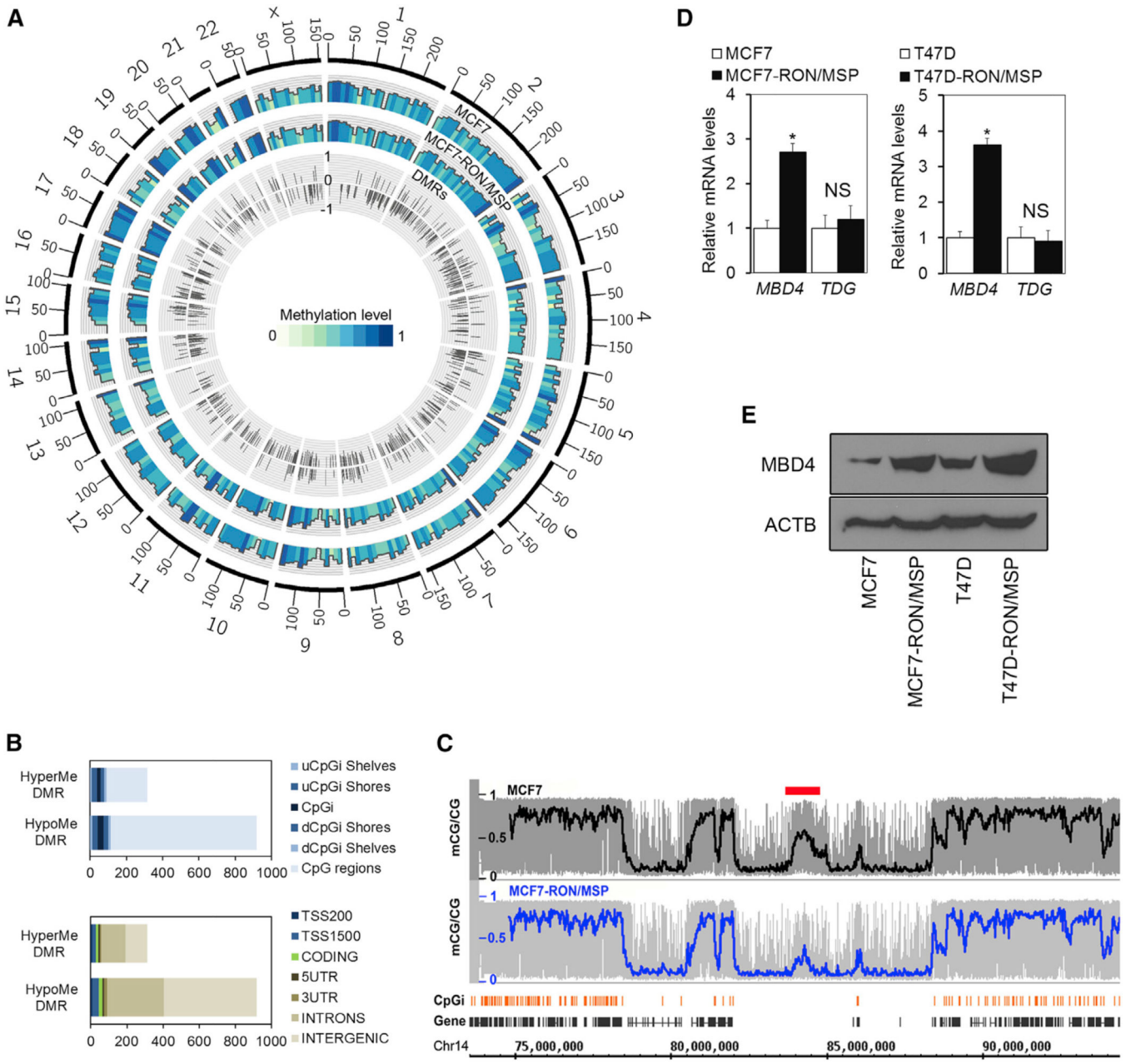

Figure 2. RON/MSP Signaling Upregulates MBD4 and Drives Aberrant DNA Methylation

(A) Circular representation of genome-wide aberrant DNA methylation caused by RON/MSP expression. Average methylation levels for all of the CGs in 10 Mbp wide windows are shown in the blue-green tracks (the outermost track shows MCF7 cells; the middle track shows MCF7-RON/MSP cells). The innermost track indicates the differentially methylated regions (DMRs) between MCF7 and MCF7-RON/MSP cells (false discovery rate >20; differential methylation >0.25). This diagram for visualization of genome-wide DNA methylation was generated using the Circos software (Krzywinski et al., 2009).

(B) Top, distribution of differentially methylated CpGs on CpG islands (CpGi) shelves (>2–4 kb from island edge) and on CpGi shores (0–2 kb from island edge), within and outside

CpGi. u, upstream of CpGi; d, downstream of CpGi. Bottom, distribution of differentially methylated CpGs across regions of other significance. TSS 200, within the region 1–200 bp upstream of the TSS; TSS 1500, within the region 201–1,500 bp upstream of the transcription start site (TSS); UTR, untranslated region; HyperMe, hypermethylated; HypoMe, hypomethylated.

(C) Example of smoothed methylation levels from bisulfite sequencing data for MCF7 (black) and MCF7-RON/MSP (blue) on chromosome 14. A hypomethylation block is indicated by a red bar.

(D) Real-time quantitative RT-PCR data showing *MBD4* and *TDG* mRNA expression levels, normalized to β-*ACTIN* mRNA levels, in MCF7, MCF7-RON/MSP, T47D, and T47D-RON/MSP cells (*$p < 0.001$).

(E) Western blot with anti-MBD4 showing upregulation of MBD4 protein expression in MCF7-RON/MSP and T47D-RON/MSP cells compared to parental MCF7 and T47D cells (fold change = 5 for MCF7 and fold change = 3 for T47D, $p < 0.001$, as quantified by ImageJ).

See also Figure S2.

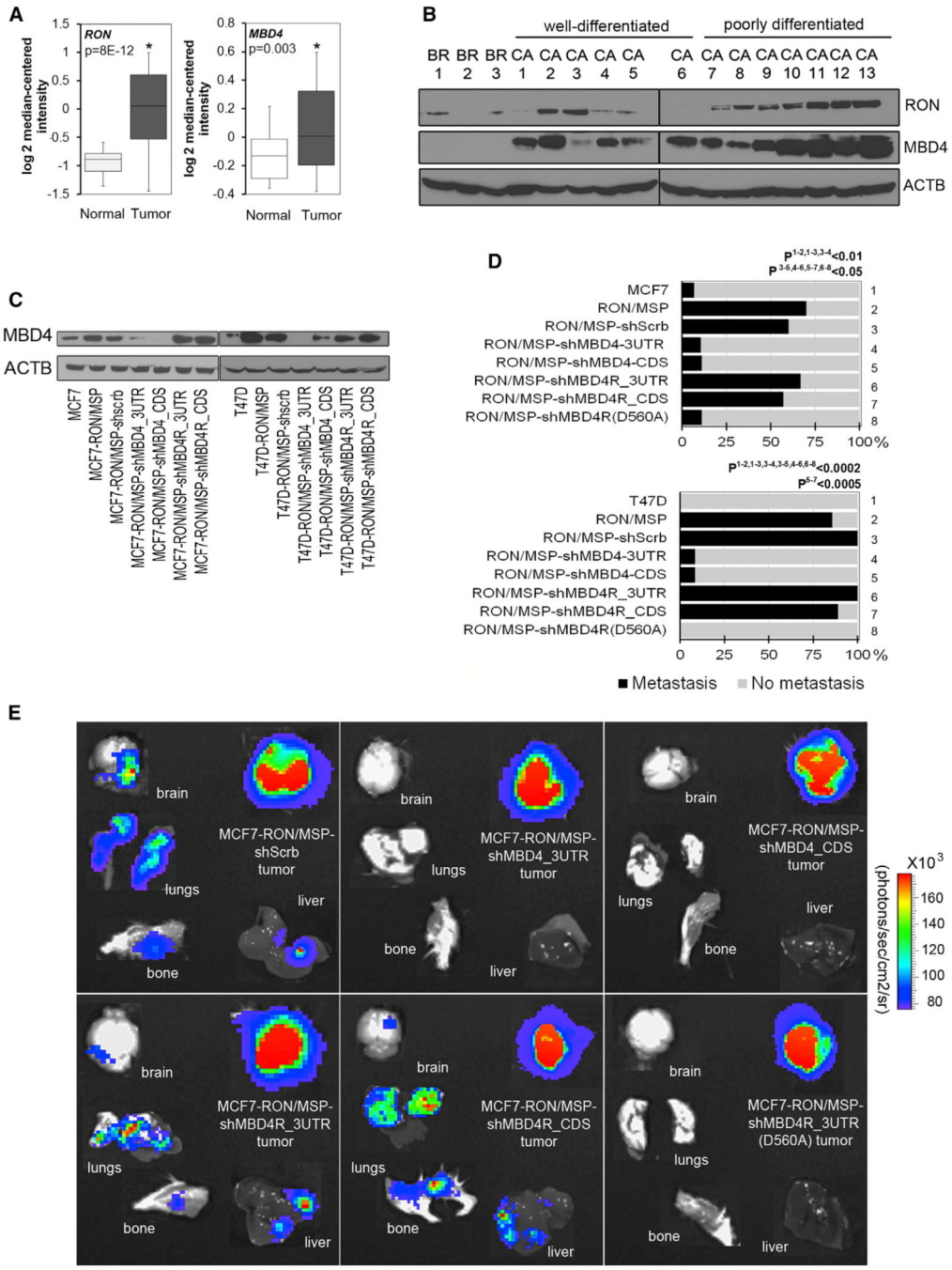

Figure 3. Knockdown of MBD4 Blocks RON/MSP-Mediated Breast Cancer Metastasis

(A) Box plot showing *RON* and *MBD4* mRNA expression in normal breast tissues (white) and breast tumors (dark gray) from The Cancer Genome Atlas (TCGA) data set.

(B) Western blot for RON and MBD4 proteins in normal human breast tissues from reduction mammoplasties and human primary breast tumor specimens; the β-actin (ACTB) loading control is also shown.

(C) Successful knockdown of MBD4 expression, shown by western blot on protein lysates from MCF7-RON/MSP-shMBD4 cells (shRNA directed to the 3’ UTR or CDS) and T47D-

RON/MSP-shMBD4 cells compared with controls (MCF7-RON/MSP, T47D-RON/MSP, and shRNA scramble control, shScrb). MBD4 re-expression following introduction of rescue cDNA into shMBD4-expressing cells (shMBD4R_3UTR and shMBD4R_CDS) is also shown for both cell lines. β-ACTIN (ACTB) levels are shown as a loading control.

(D) Top, metastasis frequencies for MCF7 parental tumors (n = 15), MCF7-RON/MSP tumors (n = 20), or tumors arising from MCF7 cells infected with RON/MSP and shScrb (n = 10), sh-MBD4-3UTR (n = 19), or shMBD4-CDS (n = 9). The effects of rescue constructs (shMBD4R_3UTR [n = 6], shMBD4R_CDS [n = 14], or the catalytic mutant shMBD4R [D560A] [n = 9]) are shown at the bottom. Bottom, metastasis frequencies for T47D parental tumors (n = 16), T47D-RON/MSP tumors (n = 14), or tumors arising from T47D cells infected with RON/MSP and shScrb (n = 7), sh-MBD4-3UTR (n = 12), or shMBD4-CDS (n = 12). The effects of rescue constructs (shMBD4R_3UTR [n = 8], shMBD4R_CDS [n = 9], or the catalytic mutant shMBD4R [D560A] [n = 8]) are shown at the bottom.

(E) Representative bioluminescent images of lung, bone, liver, and brain metastasis from single mice illustrate the effects of shScrb, sh-MBD4, rescued MBD4, and rescued catalytic mutant on metastasis of various orthotopic MCF7 tumors.

See also Figure S3.

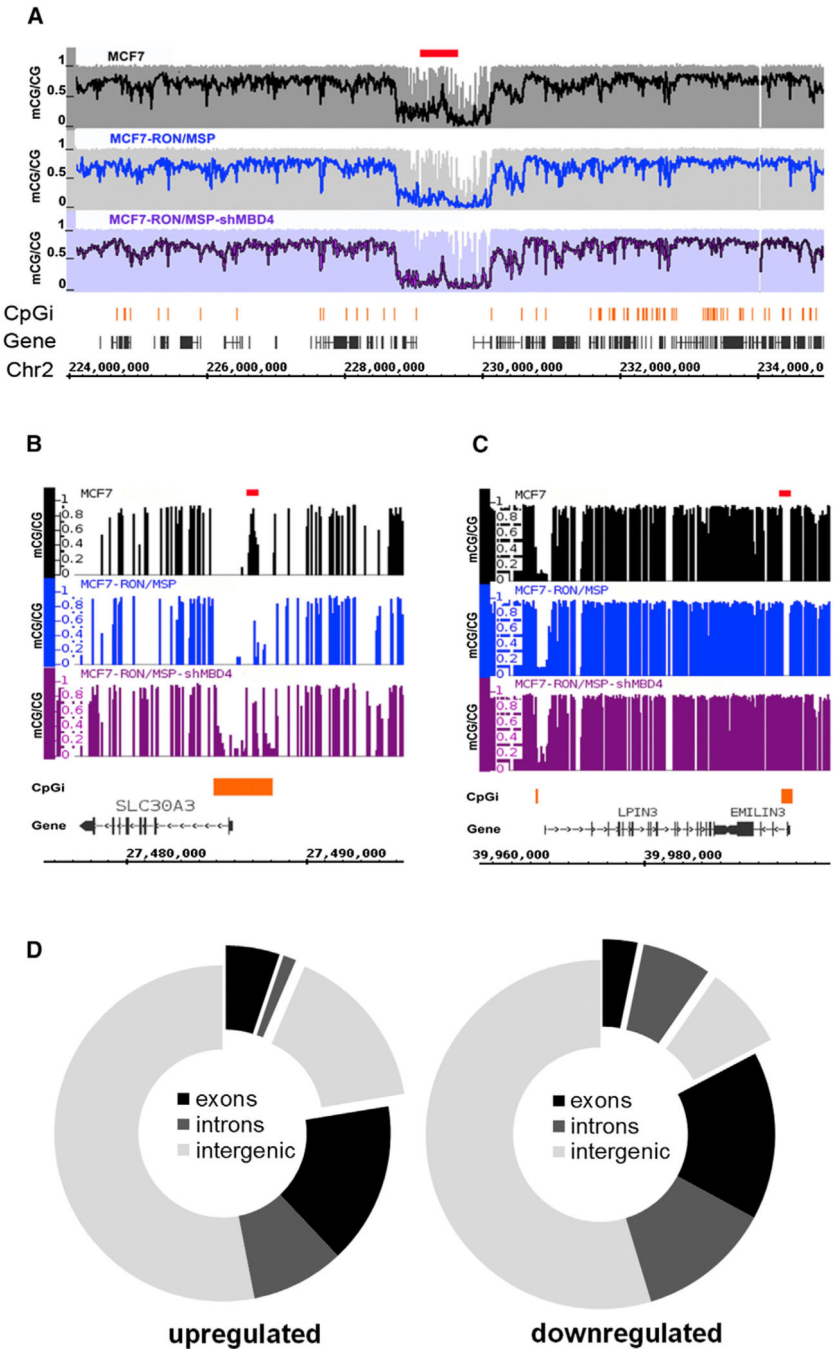

Figure 4. Knockdown of MBD4 Reverses DNA Aberrant Methylation and Expression of RON/MSP-Regulated Genes

(A) Representation of smoothed methylation values from bisulfite sequencing data for MCF7 (black), MCF7-RON/MSP (blue), and MCF7-RON/ MSP-shMBD4 cells (purple) in a representative region of chromosome 2. The hypomethylation block in MCF7-RON/MSP that becomes hypermethylated by knocking down MBD4 is indicated by a red bar.

(B) Example of DNA methylation levels in promoter regions in MCF7 (black), MCF7-RON/MSP (blue), and MCF7-RON/MSP-shMBD4 cells (purple). The hypomethylated

block in MCF7-RON/MSP cells that becomes remethylated by knocking down MBD4 is indicated by a red bar.

(C) Example of DNA methylation levels in a promoter region that becomes hypermethylated in shMBD4 cells, independent of RON/MSP expression (red bar). Bisulfite sequencing data for MCF7 (black), MCF7-RON/MSP (blue), and MCF7-RON/ MSP-shMBD4 cells (purple) are shown. In all panels, the orange bars indicate CpG islands, and the black bars show the genes.

(D) Diagrams representing the proportion of exons, introns, and intergenic regions for which expression was reversed by knocking down MBD4 (outside shifted circle).

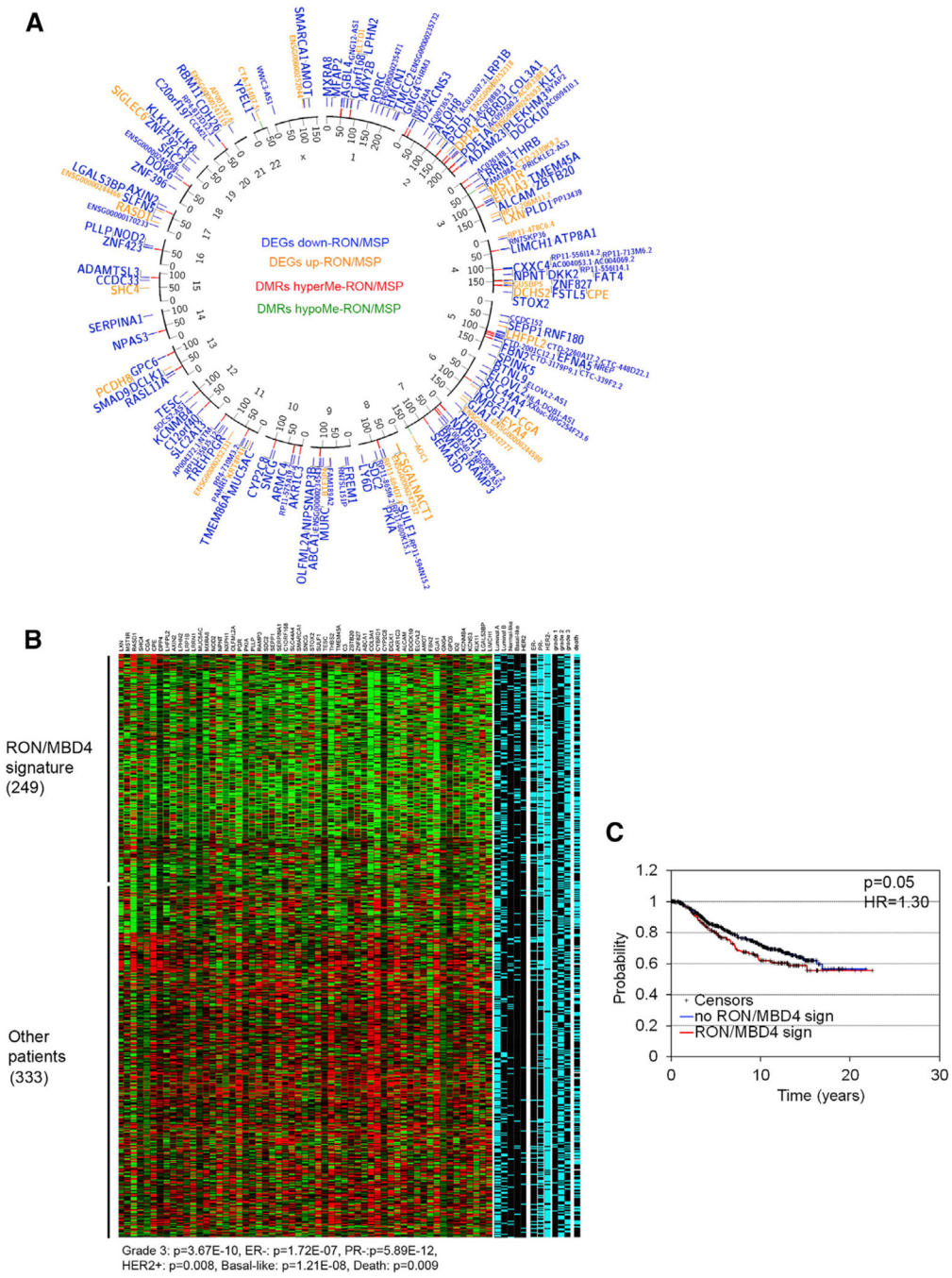

Figure 5. Specific Subclasses of Human Breast Tumors Possess the RON/MBD4 Epigenetic Signature, which Correlates with Poor Prognosis

(A) Circular representation of the RON/MBD4 epigenetic signature. The outside track represents the 192 genes regulated by RON/MSP for which expression was reversed following knockdown of MBD4 (blue, genes downregulated by RON/MSP and then reversed by knocking down MBD4 with shRNA; orange, genes upregulated by RON/MSP and then reversed by knocking down MBD4). In larger characters are the genes that are annotated in the METABRIC data set. The inner track represents the statistically significant DMRs at these regions (red, hypermethylated DMRs in MCF7-RON/MSP and then reversed

by knocking down MBD4; green, hypomethylated DMRs in MCF7-RON/MSP and then reversed by knocking down MBD4).

(B) Enrichment pattern of the gene set comprising the RON/MBD4 epigenetic signature (rows) across 997 breast tumors (columns). Red and green indicated a significantly over- or under-expressed gene, respectively. Are represented the 582 patients having enrichment or underrepresentation of the gene set. Blue bars (right) indicate individual tumor annotations for breast cancer subtype. Bottom: association of the RON/ MBD4 epigenetic signature with ER, HER2, and PR status, as well as intrinsic breast cancer subtype, grade, and death (we assigned a p value according to the hypergeometric distribution).

(C) Kaplan-Meier analysis of overall survival in 997 breast cancer patients from the METABRIC discovery data set (Curtis et al., 2012). Survival curve of individuals with tumors showing an enrichment of the 116 annotated genes from the RON/MBD4 epigenetic signature is shown in red; all other patients are shown in blue (no signature). The p value indicates a statistically significant survival difference between these two groups of patients. The survival hazard ratio was calculated using univariate Cox’s regression analysis.

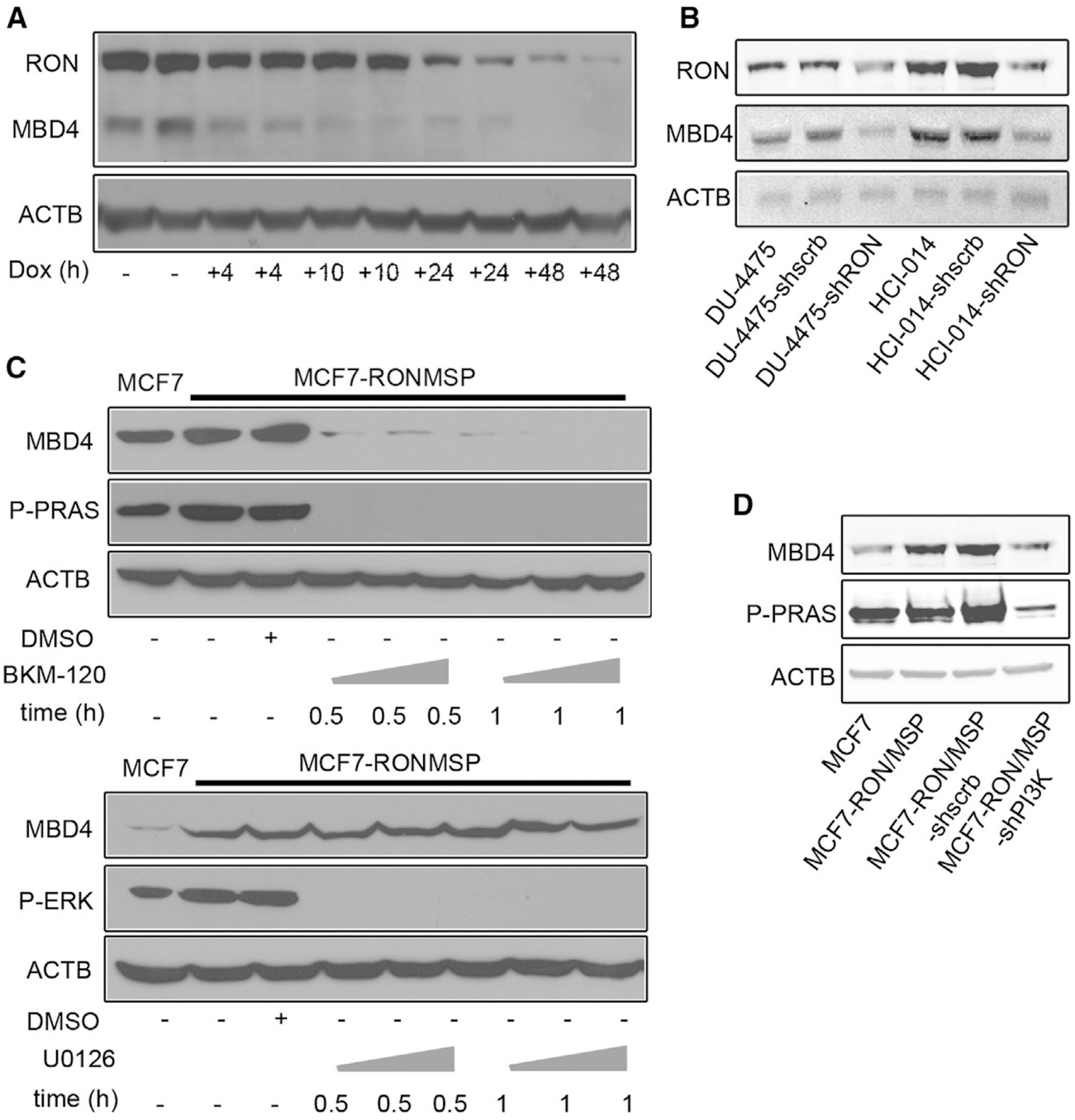

Figure 6. MBD4 Is Regulated by RON/MSP Signaling through PI3K Pathway

(A) Western blot with anti-RON, anti-MBD4, and anti-β-ACTIN on protein lysates from the MCF7-TRE-RON/MSCV-tTA cell line treated with or without (+/−) doxycycline for the indicated times (duplicate samples).

(B) Western blot showing expression of endogenous RON and MBD4 proteins in the DU-4475 breast cancer cell line and in a patient-derived breast tumor graft (HCI-014) before and after infection with lentiviruses carrying RON shRNA (fold change = 3, $p < 0.02$, and fold change = 5, $p < 0.01$, respectively, as quantified by ImageJ).

(C) Top: western blot with anti-MBD4, anti-p-PRAS, and anti-β-ACTIN in MCF7 and MCF7-RON/ MSP cells treated with DMSO or BKM-120 (50 nM, 100 nM, or 500 nM for the time indicated; fold change = 12, $p < 0.001$, as quantified by ImageJ). Bottom: western blot with anti-MBD4, anti-p-ERK, and anti- β-ACTIN in MCF7 and MCF7-RON/MSP cells treated with DMSO or U0126 (5 μM, 10 μM, or 50 μM for the time indicated).
(D) Western blot showing the expression of MBD4 and p-PRAS in MCF7 and MCF7-RON/MSP cells infected with lentiviruses carrying PI3K–p110 shRNA or scrambled shRNA control (fold change = 2, $p < 0.01$, as quantified by ImageJ).
See also Figure S4.

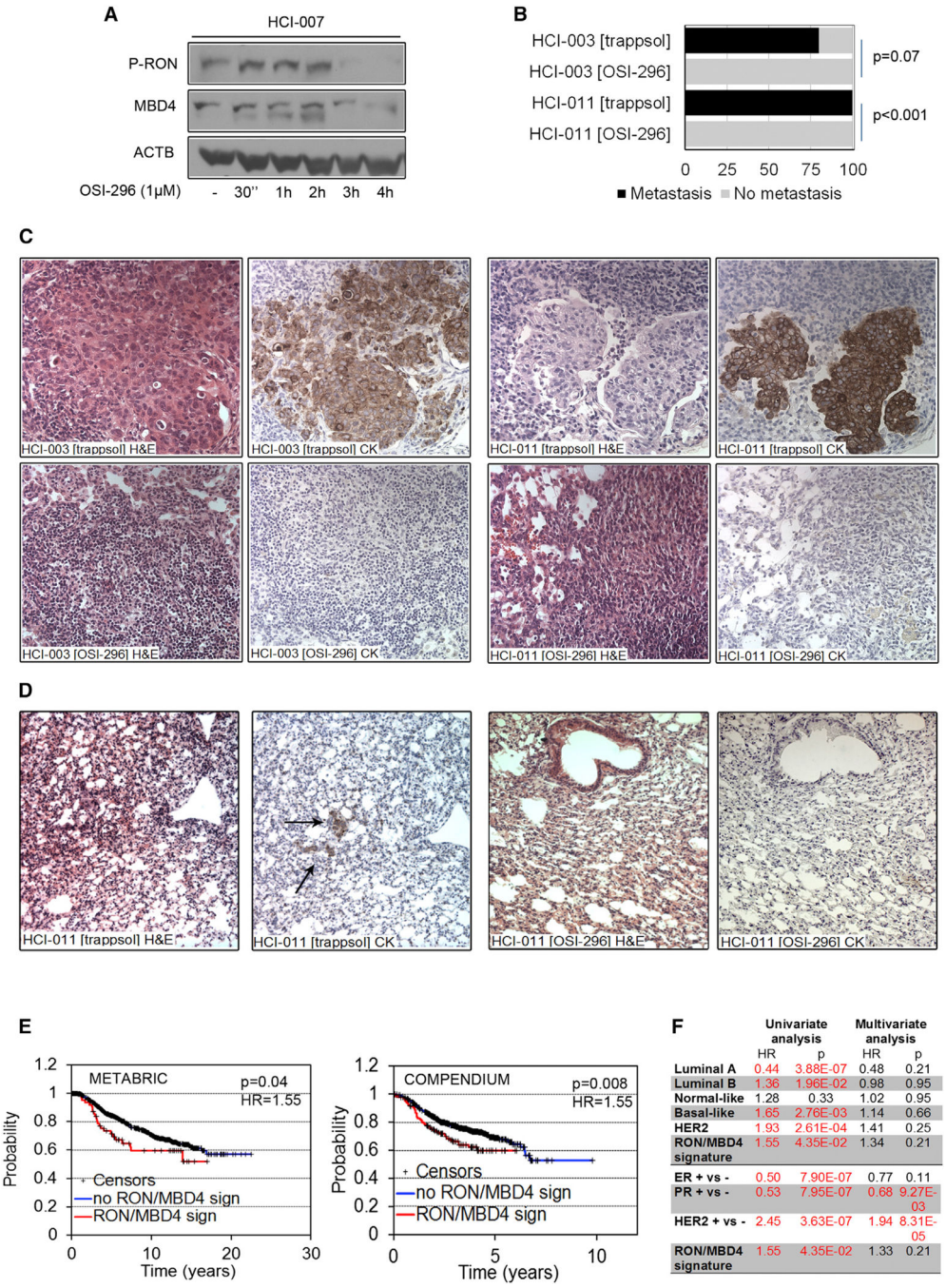

	Univariate analysis		Multivariate analysis	
	HR	p	HR	p
Luminal A	0.44	3.88E-07	0.48	0.21
Luminal B	1.36	1.96E-02	0.98	0.95
Normal-like	1.28	0.33	1.02	0.95
Basal-like	1.65	2.76E-03	1.14	0.66
HER2	1.93	2.61E-04	1.41	0.25
RON/MBD4 signature	1.55	4.35E-02	1.34	0.21
ER + vs -	0.50	7.90E-07	0.77	0.11
PR + vs -	0.53	7.95E-07	0.68	9.27E-03
HER2 + vs -	2.45	3.63E-07	1.94	8.31E-05
RON/MBD4 signature	1.55	4.35E-02	1.33	0.21

Figure 7. Treatment with a RON Inhibitor, OSI-296, Drastically Decreases Breast Cancer Metastasis in Human-Patient-Derived Breast Tumor Grafts

(A) Western blots with p-RON, MBD4, and β-ACTIN antibodies on protein lysates from primary cultures of the patient-derived tumor graft HCI-007, treated without (−) or with 1 μM of the RON inhibitor OSI-296 over the indicated times.

(B) Metastasis frequencies for orthotopically implanted patient-derived tumor grafts HCI-003 and HCI-011 following treatment with OSI-296 (n = 3 and n = 9, for HCI-003 and HCI-011, respectively) ortrappsol (n = 5 for both HCI-003 and HCI-011) vehicle control (p value determined by Fisher's exact test).

(C) Sections of axillary lymph nodes isolated from mice carrying orthotopic (inguinal fat pad) patient-derived breast tumor grafts HCI-003 and HCI-011 following treatment with trappsol orOSI-296. The sections were stained with H&E (left) orwere immunostained with antibodies specific for human cytokeratin (right) in order to detect human tumor cells.
(D) Sections of lungs isolated from mice carrying orthotopic patient-derived breast tumor grafts HCI-011 following treatment with trappsol or OSI-296. The sections were stained with H&E (left) or were immunostained with antibodies specific for human cytokeratin (CK; right) to identify human tumor cells.
(E) Kaplan-Meier analysis of overall survivalin 997 breastcancer patients from the METABRIC discovery data set (left, Curtis et al., 2012) and in 977 breast cancer patients from the compendium data set (right, van ‘t Veer et al., 2002; Miller et al., 2005; Chin et al., 2006; Desmedt et al., 2007; Heikkinen et al., 2011). Survival curve of individuals with tumors showing an enrichment of the nine RON/MBD4 epigenetic signature genes that were deregulated in tumors from mice treated with OSI-296 compared to the trappsol control is shown in red; all other patients are shown in blue (no signature). The p value indicates a statistically significant survival difference between these two groups of patients. The survival hazard ratio was calculated using univariate Cox’s regression analysis.
(F) Univariate and multivariate cox regression analyses for overall survival in the 997 patients from the METABRIC data set, examining ER, PR, status, basal-like subtype, and the MBD4/RON signature as variables. HR, hazard ratio.